Chinese Physics C Vol. 50, No. 10 (2026) 103109

Lesser Green's function and chirality-reduced entropy via the In-Medium NJL model*

Seung-il Nam†

Department of Physics, Pukyong National University (PKNU), Busan 48513, Republic of Korea and Asia Pacific Center for Theoretical Physics (APCTP), Pohang 37673, Korea

Abstract: We investigate chiral symmetry restoration in finite-temperature and finite-density quark matter using a correlator-based chirality-reduced entropy within the in-medium Nambu–Jona-Lasinio (NJL) model. Starting from the lesser Green's function $G^{<}(k)$ in the real-time formalism, we construct the equal-time correlation matrix $C(\boldsymbol{k})$ and define the left-handed reduced correlator $C_L(\boldsymbol{k}) = P_L C(\boldsymbol{k}) P_L$. The corresponding von Neumann entropy, $S_\chi = -\mathrm{Tr}[C_L \ln C_L + (1-C_L)\ln(1-C_L)]$, characterizes the mixedness of the chirality-reduced subsystem. We show that the reduced correlator retains a nontrivial helicity structure and therefore must be described by its full eigenvalue spectrum rather than by a single scalar occupation probability. The self-consistent dynamical quark mass $M_q(T,\mu_q)$ reproduces the expected QCD-like phase structure, with a second-order transition in the chiral limit and a smooth crossover for finite current quark mass. The chirality-reduced entropy correlates with chiral restoration but is not an order parameter; instead, it provides complementary information through the full spectrum of the reduced correlator. Our numerical results show that S_χ exhibits characteristic nontrivial behavior across the chiral transition region and serves as an information-theoretic diagnostic of reduced chiral-sector mixedness.

Keywords: chiral symmetry restoration, Nambu–Jona-Lasinio model, von Neumann entropy, chirality-reduced entropy, lesser Green's function, quantum information in QCD

DOI: 10.1088/1674-1137/ae8825 **CSTR:** 32044.14.ChinesePhysicsC.50103109

I. INTRODUCTION

Spontaneous chiral symmetry breaking (SCSB) and the restoration of chiral symmetry are central aspects of Quantum Chromodynamics (QCD), playing key roles in hadron mass generation and in the formation of the quark–gluon plasma (QGP) at high temperatures or densities [1−5]. In the QCD vacuum, chiral symmetry is dynamically broken, leading to a large constituent quark mass and the emergence of light pseudoscalar mesons as Nambu–Goldstone bosons. As the temperature or baryon density increases, the quark condensate $\langle\bar{q}q\rangle$ melts, the constituent mass decreases, and chiral symmetry is partially restored. Lattice QCD simulations indicate that, for physical quark masses, this restoration occurs through a smooth crossover at vanishing chemical potential [6, 7]. Effective approaches, such as the Nambu–Jona-Lasinio (NJL), Polyakov-NJL (PNJL), and instanton-based models, reproduce the qualitative features of the QCD phase diagram [2, 3, 8−10].

Recent developments have applied concepts from quantum information theory to strongly interacting systems, using entropy-based observables to characterize correlations and mixedness [11−14]. In QCD and related field theories, such ideas have been explored in connection with confinement, deconfinement, topology, spin structures, and high-energy observables. Examples include entanglement entropy in deep-inelastic scattering, entropy production in hadronic final states, and QCD evolution of entanglement-related quantities [15−20]. These developments demonstrate that information-theoretic quantities can provide useful probes of correlations that are not always directly accessible through conventional local order parameters.

The present work differs from studies based on spatial bipartite entropy, small-x partonic entropy, or color-sector entropy. We instead focus on an internal chiral reduction of the fermionic equal-time correlator. Starting from the real-time lesser Green's function, we construct the correlator $C(k)$, project it onto the left-handed sub-

Received 25 February 2026; Accepted 8 July 2026; Accepted manuscript online 9 July 2026

* Supported by a National Research Foundation of Korea (NRF) grant funded by the Korean government (MSIT) (RS-2025-16065906)

† E-mail: sinam@pknu.ac.kr

space as $C_L(k) = P_L C(k) P_L$, and define the chirality-reduced entropy from the eigenvalue spectrum of $C_L(k)$. Thus, S_χ is designed to quantify the mixedness of a chirality-reduced Gaussian subsystem. It is correlated with chiral restoration, but it is not an order parameter and should not be identified with the chiral condensate or the dynamical quark mass. In this sense, the present correlator-based entropy provides a perspective complementary to conventional symmetry-based observables.

In this work, we investigate chiral symmetry restoration in hot and dense quark matter using a correlator-based chirality-reduced entropy within the in-medium NJL model. Starting from the lesser Green's function $G^<(k)$ in the real-time formalism [21, 22], we construct the equal-time correlation matrix.

$$C(\boldsymbol{k}) = \mathrm{i}\int \frac{\mathrm{d}k^0}{2\pi} G^<(k), \tag{1}$$

and define the left-handed reduced correlator as $C_L(\boldsymbol{k}) = P_L C(\boldsymbol{k}) P_L$. The corresponding von Neumann entropy,

$$S_\chi = -\mathrm{Tr}\left[C_L \ln C_L + (1-C_L)\ln(1-C_L)\right]. \tag{2}$$

This quantity is used to quantify the mixedness of the chirality-reduced subsystem.

Within the mean-field NJL framework, the reduced correlator retains a nontrivial helicity structure and must therefore be characterized by its full eigenvalue spectrum rather than by a single scalar occupation probability. The self-consistent dynamical quark mass $M_q(T,\mu_q)$ reproduces the expected QCD-like phase structure, with a second-order transition in the chiral limit and a smooth crossover for a finite current quark mass. The resulting entropy is correlated with chiral restoration but is not an order parameter; rather, it reflects the structure of the reduced correlator beyond local one-point observables.

Conceptually, this quantity differs from the conventional chiral condensate $\langle\bar{q}q\rangle$. Whereas the condensate is a local expectation value that characterizes the magnitude of symmetry breaking, S_χ is defined through the spectrum of a reduced fermionic correlation matrix restricted to a chiral subspace. It therefore characterizes the mixedness of the chiral sector rather than the strength of symmetry breaking itself.

Most existing entropy-related studies in QCD focus on spatial bipartite entropy, Rényi entropies, or color-sector observables in Euclidean or lattice formulations. In contrast, the present work considers an entropy associated with an internal chiral degree of freedom, constructed from the real-time lesser Green's function through the corresponding equal-time correlator. This provides a complementary probe of chiral dynamics that is not directly captured by conventional symmetry-breaking observables.

This paper is organized as follows. In Sec. II, we outline the finite-temperature NJL framework and the real-time formalism for the lesser Green's function. In Sec. III, we construct the equal-time correlator and derive the chirality-reduced correlator. Section IV presents the reduced correlator in the chiral basis and its eigenvalue structure. In Sec. V, we introduce the von Neumann chirality-reduced entropy and discuss its interpretation. Numerical results are presented in Sec. VI, followed by conclusions in Sec. VII.

II. IN-MEDIUM NJL MODEL

The Nambu–Jona-Lasinio (NJL) model provides an effective description of dynamical chiral symmetry breaking through a chirally symmetric four-fermion interaction. Its Lagrangian is given by

$$\mathcal{L}_{\mathrm{NJL}} = \bar{q}(\mathrm{i}\gamma^\mu\partial_\mu - m_q)q + G\left[(\bar{q}q)^2 + (\bar{q}\mathrm{i}\gamma_5\boldsymbol{\tau}q)^2\right]. \tag{3}$$

Here, $q=(u,d)^T$ denotes the light quark fields, m_q is the current-quark mass, and G is the coupling constant. The interaction term preserves the global $SU(2)_L\times SU(2)_R$ symmetry in the chiral limit.

In the present work, we employ the minimal two-flavor NJL model with scalar and pseudoscalar interactions. This choice isolates the role of the dynamically generated constituent mass in the chirality-reduced correlator and the associated entropy. Additional interaction channels, such as vector interactions, primarily modify the medium dependence and are not essential to the mechanism considered here.

Dynamical mass generation arises through the formation of a quark condensate, which gives rise to the constituent quark mass

$$M_q = m_q - 2G\langle\bar{q}q\rangle, \tag{4}$$

which is determined self-consistently from the finite-temperature gap equation,

$$\begin{aligned} M_q(T,\mu_q) &= m_q - 2G\langle\bar{q}q\rangle, \\ \langle\bar{q}q\rangle &= -4N_cN_f\int_0^\Lambda \frac{\mathrm{d}^3\vec{k}}{(2\pi)^3}\frac{M_q}{E_k}\left[1-n_+-n_-\right], \end{aligned} \tag{5}$$

where $E_k^2 = |\vec{k}|^2 + M_q^2$ and the Fermi–Dirac distribution functions are given by

$$n_F(E_k\pm\mu_q) = \frac{1}{\mathrm{e}^{(E_k\pm\mu_q)/T}+1} \equiv n_\mp. \tag{6}$$

The NJL parameter set employed in this work is listed in Table 1.

Figure 1 shows the temperature and chemical-potential dependence of the dynamical quark mass $M_q(T,\mu_q)$ obtained from Eq. (5). In the chiral limit ($m_q=0$), the constituent mass decreases continuously with temperature at $\mu_q=0$, indicating a second-order transition. At higher quark chemical potential, the transition becomes first order, with a critical end point separating the two regimes.

For a finite current quark mass ($m_q=5.25$ MeV), chiral symmetry is explicitly broken, and the phase transition is replaced by a smooth crossover. In this case, M_q decreases gradually with increasing temperature and density, while remaining finite even at high temperatures. This behavior is consistent with lattice QCD results and confirms that the NJL model captures the qualitative features of chiral symmetry restoration.

Varying the model parameters within reasonable ranges, $\Lambda=(630\pm30)\,\mathrm{MeV}$ and $G\Lambda^2=2.1\pm0.1$, was found to modify only the overall magnitude of the results, without affecting their qualitative behavior or the location of the pseudo-critical region. This finding confirms the robustness of the present analysis.

III. LESSER GREEN'S FUNCTION AND CHIRAL CORRELATOR FRAMEWORK

In the Schwinger–Keldysh real-time formalism [22], the greater and lesser Green's functions are defined as

$$G^{>}(x,y)=-\mathrm{i}\langle q(x)\bar{q}(y)\rangle,\quad G^{<}(x,y)=\mathrm{i}\langle\bar{q}(y)q(x)\rangle. \tag{7}$$

Table 1. The NJL parameter set used in the present study.

m_q /MeV	Λ /MeV	$G\Lambda^2$
5.25	631.4	2.14

In equilibrium, they are related to the spectral function $A(p)=\mathrm{i}\left[G^R(p)-G^A(p)\right]$ and to the Fermi distribution $n_F(p^0)$ by

$$G^{<}(p)=\mathrm{i}\,n_F(p^0)A(p),\quad G^{>}(p)=-\mathrm{i}\,[1-n_F(p^0)]A(p). \tag{8}$$

Thus, $G^{<}(p)$ encodes the occupied component of the spectral density. However, in the Gaussian entropy construction, the relevant quantity is the equal-time correlation matrix rather than $G^{<}(k)$ itself

$$C(\boldsymbol{k})\equiv\mathrm{i}\int\frac{\mathrm{d}k_0}{2\pi}G^{<}(k), \tag{9}$$

whose eigenvalues are contained in the interval $[0,1]$.

In the mean-field NJL model, the lesser propagator takes the form

$$G^{<}(k)=2\pi\mathrm{i}\left[n_+\Lambda_+(\boldsymbol{k})\delta(k_0-E_k)+(1-n_-)\Lambda_-(\boldsymbol{k})\delta(k_0+E_k)\right], \tag{10}$$

where $E_k=\sqrt{\boldsymbol{k}^2+M_q^2}$, and $n_\pm=n_F(E_k\mp\mu_q)$. The positive- and negative-energy projectors are

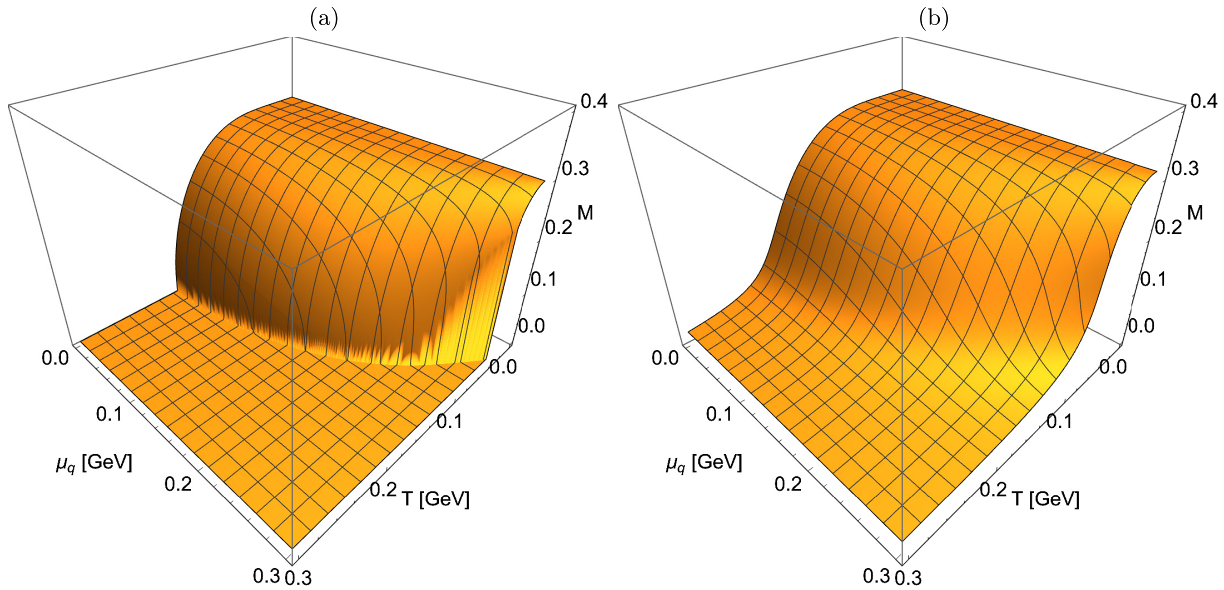

Fig. 1. (color online) Dynamical quark mass M_q as a function of temperature T and quark chemical potential μ_q for $m_q=0$ (a) and $m_q=$ 5.25 MeV (b).

$$\Lambda_\pm(\boldsymbol{k}) = \frac{1}{2}\left[1 \pm \frac{\gamma^0(\boldsymbol{\gamma}\cdot\boldsymbol{k}+M_q)}{E_k}\right], \tag{11}$$

with

$$\Lambda_\pm^2 = \Lambda_\pm, \quad \Lambda_+\Lambda_- = 0, \quad \Lambda_+ + \Lambda_- = 1. \tag{12}$$

Integrating Eq. (10) over k_0 yields the equal-time correlator.

$$C(\boldsymbol{k}) = n_+\Lambda_+(\boldsymbol{k}) + [1-n_-]\Lambda_-(\boldsymbol{k}). \tag{13}$$

This correlator provides the starting point for the chirality-reduced construction developed below.

In the chiral limit $M_q \to 0$, the Dirac Hamiltonian becomes block-diagonal with respect to chirality, and the left- and right-handed sectors decouple dynamically. For nonzero M_q, the Dirac mass term mixes the two chiral sectors through the off-diagonal structure of the Dirac operator in the Weyl basis. Accordingly, $C(\boldsymbol{k})$ contains information about both thermal occupation and mass-induced left–right mixing. Detailed derivations are provided in Appendices A and B.

IV. CHIRALITY DECOMPOSITION AND REDUCED CORRELATOR

A Dirac field can be decomposed into left- and right-handed components as

$$q = q_L + q_R, \quad q_{L,R} = P_{L,R}q,$$
$$P_{L,R} = \frac{1\mp\gamma^5}{2}. \tag{14}$$

In the chiral limit $M_q \to 0$, the two sectors dynamically decouple, whereas a finite constituent mass induces left–right mixing.

To quantify the reduced left-handed sector, we define the chirality-projected equal-time correlator

$$C_L(\boldsymbol{k}) = P_L C(\boldsymbol{k}) P_L = n_+ P_L\Lambda_+(\boldsymbol{k})P_L + (1-n_-)P_L\Lambda_-(\boldsymbol{k})P_L. \tag{15}$$

In the Weyl basis, the projectors have the block form

$$\Lambda_\pm(\boldsymbol{k}) = \frac{1}{2}\begin{pmatrix} I \mp \dfrac{\boldsymbol{\sigma}\cdot\boldsymbol{k}}{E_k} & \pm\dfrac{M_q}{E_k} \\ \pm\dfrac{M_q}{E_k} & I \pm \dfrac{\boldsymbol{\sigma}\cdot\boldsymbol{k}}{E_k}\end{pmatrix}. \tag{16}$$

Projection onto the left-handed subspace yields

$$P_L\Lambda_+P_L = \frac{1}{2}\left(I - \frac{\boldsymbol{\sigma}\cdot\boldsymbol{k}}{E_k}\right)P_L, \quad P_L\Lambda_-P_L = \frac{1}{2}\left(I + \frac{\boldsymbol{\sigma}\cdot\boldsymbol{k}}{E_k}\right)P_L. \tag{17}$$

Substituting this into Eq. (15) yields

$$C_L(\boldsymbol{k}) = a_k I + b_k\,\boldsymbol{\sigma}\cdot\hat{\boldsymbol{k}}, \tag{18}$$

with

$$a_k = \frac{1}{2}(1+n_+-n_-), \quad b_k = \frac{|\boldsymbol{k}|}{2E_k}(1-n_--n_+). \tag{19}$$

The eigenvalues are therefore

$$\lambda_\pm(\boldsymbol{k}) = a_k \pm b_k, \quad \Delta\lambda(\boldsymbol{k}) \equiv \lambda_+(\boldsymbol{k}) - \lambda_-(\boldsymbol{k}) = 2b_k. \tag{20}$$

These eigenvalues satisfy $0 \le \lambda_\pm \le 1$. Hence, the reduced correlator is characterized by its full eigenvalue spectrum rather than by a single scalar occupation probability. In particular, for finite M_q, the vacuum limit does not generically yield $\lambda_\pm = 0, 1$ on a mode-by-mode basis.

Figure 2 shows the eigenvalue splitting $\Delta\lambda(\boldsymbol{k}) = 2b_k$ as a function of temperature and momentum. At low temperatures, the splitting remains substantial over a broad momentum range, indicating well-separated eigenmodes. As the temperature increases, thermal broadening drives the system toward $\lambda_+ = \lambda_- = \frac{1}{2}$, such that $\Delta\lambda \to 0$, reflecting the increased mixed character of the reduced subsystem. Finite density modifies the temperature dependence of the splitting while preserving this overall trend.

Table 2 presents the limiting forms of the eigenvalues $\lambda_\pm(\boldsymbol{k})$ and their splitting $\Delta\lambda$ in several important limits. In the chiral limit $M_q \to 0$, one finds $\lambda_\pm(\boldsymbol{k}) = \{1-n_-, n_+\}$ and $\Delta\lambda = 1-n_--n_+$. In the asymptotically high-temperature limit $T\to\infty$, both eigenvalues approach $1/2$, implying a vanishing splitting, $\Delta\lambda = 0$. In the vacuum limit $(T,\mu_q)\to(0,0)$, the eigenvalues reduce to $\lambda_\pm(\boldsymbol{k}) = (1\pm|\boldsymbol{k}|/E_k)/2$, so that $\Delta\lambda = |\boldsymbol{k}|/E_k$. Thus, the table concisely summarizes how the eigenvalue spectrum changes across different physical regimes.

V. VON NEUMANN ENTROPY AND CHIRALITY-REDUCED ENTROPY

The von Neumann entropy of the left-handed reduced subsystem is defined in terms of the equal-time correlator C_L as

$$S_\chi = -\mathrm{Tr}\left[C_L\ln C_L + (1-C_L)\ln(1-C_L)\right]. \tag{21}$$

For a Gaussian fermionic state, this quantity is determ-

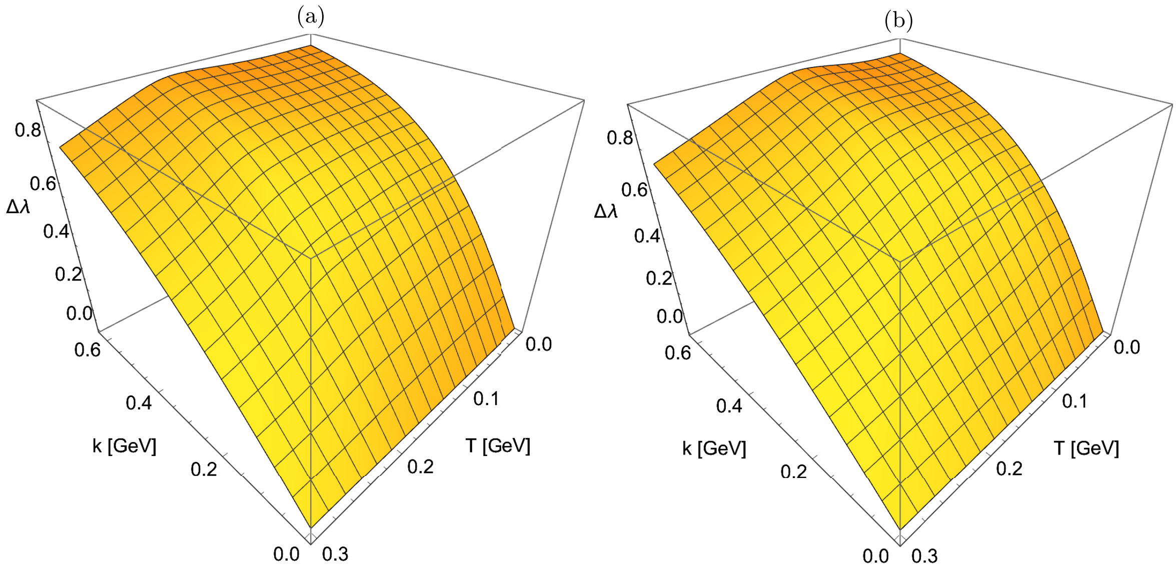

Fig. 2. (color online) Eigenvalue splitting of the chirality-reduced correlator, $\Delta\lambda(\boldsymbol{k})=\lambda_+(\boldsymbol{k})-\lambda_-(\boldsymbol{k})$, as a function of temperature T and momentum $|\boldsymbol{k}|$ for $\mu_q=0$ (a) and 200 MeV (b), with $m_q\neq 0$.

Table 2. Limiting forms of the eigenvalues $\lambda_\pm(\boldsymbol{k})$ and of their splitting $\Delta\lambda$.

Limit	$\lambda_\pm(\boldsymbol{k})$	$\Delta\lambda$
$M_q\to 0$	$\{1-n_-,n_+\}$	$1-n_--n_+$
$T\to\infty$	$\frac{1}{2}$	0
$(T,\mu_q)\to(0,0)$	$\frac{1}{2}\left(1\pm\frac{\lvert\boldsymbol{k}\rvert}{E_k}\right)$	$\frac{\lvert\boldsymbol{k}\rvert}{E_k}$

ined entirely by the eigenvalues of C_L. At finite temperature and chemical potential, it quantifies the mixedness of the left-handed subsystem and generally includes both quantum and thermal contributions. Therefore, it is more appropriate to interpret S_χ as a chirality-reduced entropy (or chirality-subsystem entropy) rather than as an unqualified entanglement entropy.

Using Eq. (21), the entropy density becomes

$$\frac{S_\chi}{V}=N_cN_f\int_0^\Lambda\frac{\mathrm{d}^3k}{(2\pi)^3}\sum_{h=\pm}[-\lambda_h(\boldsymbol{k})\ln\lambda_h(\boldsymbol{k}) -(1-\lambda_h(\boldsymbol{k}))\ln(1-\lambda_h(\boldsymbol{k}))],\tag{22}$$

and the corresponding single-mode entropy is

$$s_\chi(\boldsymbol{k})=-\sum_{h=\pm}[\lambda_h(\boldsymbol{k})\ln\lambda_h(\boldsymbol{k})+(1-\lambda_h(\boldsymbol{k}))\ln(1-\lambda_h(\boldsymbol{k}))].\tag{23}$$

The entropy vanishes only when the eigenvalues take idempotent values, $\lambda_h=0$ or 1, and is maximized when $\lambda_+=\lambda_-=\frac{1}{2}$. In the high-temperature limit, $n_\pm\to\frac{1}{2}$, implying $\lambda_\pm\to\frac{1}{2}$; consequently, the entropy reaches its maximum thermal value. By contrast, in the vacuum limit $T\to 0$ and $\mu_q=0$,

$$\lambda_\pm(\boldsymbol{k})=\frac{1}{2}\left(1\pm\frac{|\boldsymbol{k}|}{E_k}\right),\tag{24}$$

which is generally non-idempotent for finite M_q. Therefore, the chirality-reduced entropy does not necessarily vanish in the zero-temperature vacuum state.

We emphasize that S_χ cannot be expressed as a functional of the chiral condensate $\langle\bar{q}q\rangle$ alone. The condensate is a local scalar expectation value that characterizes the magnitude of symmetry breaking, whereas S_χ depends on the full spectrum of the reduced correlator $C_L(\boldsymbol{k})$. Thus, it encodes information about the mixedness of the reduced chiral sector that is not contained in conventional local order parameters.

Accordingly, the behavior of $S_\chi(T,\mu_q)$ should be interpreted in terms of the temperature- and density-dependent mixedness of the chirality-reduced subsystem. Although it is correlated with chiral restoration, it should not be identified as a pure entanglement measure unless thermal contributions are removed using an appropriate mixed-state entanglement diagnostic.

Before proceeding, we clarify the approximations underlying the present construction. The NJL interaction is treated at the mean-field level, so the four-fermion operator is replaced by a self-consistent constituent mass obtained from the gap equation. In the real-time formalism, we further employ the narrow-width quasiparticle approximation for the spectral function, so that the lesser propagator takes the on-shell form in Eq. (10). The entropy is then computed from the equal-time correlation matrix of the corresponding Gaussian fermionic state. Hence, the present S_χ quantifies the mixedness of the chirality-reduced Gaussian subsystem determined by the two-point correlator. Beyond mean-field, finite spectral widths and non-Gaussian correlations may quantitatively modify the entropy and require a more general treatment.

VI. NUMERICAL RESULTS AND DISCUSSION

We now discuss the numerical behavior of the chirality-reduced entropy S_χ obtained from Eq. (22), along with the temperature and density dependence of the dynamical quark mass $M_q(T,\mu_q)$ determined from the NJL gap equation. The finite low-temperature baseline of S_χ is consistent with the reduced-state interpretation developed in Sec. V: even in the vacuum limit, the chirality-reduced correlator generally remains non-idempotent for finite M_q, so the reduced entropy does not vanish mode by mode.

Figure 3 shows S_χ as a function of temperature T and quark chemical potential μ_q for both the chiral limit ($m_q = 0$) and the physical current-mass case ($m_q = 5.25$ MeV). In both cases, S_χ exhibits nontrivial evolution across the chiral transition region. At sufficiently high temperature, the entropy increases because thermal broadening drives the eigenvalues $\lambda_\pm(\boldsymbol{k})$ toward 1/2, thereby enhancing the mixedness of the chirality-reduced subsystem.

A characteristic feature of Fig. 3 is that, at fixed μ_q, S_χ is not monotonic over the entire temperature range. In particular, for sufficiently large μ_q, the entropy is suppressed in the low-temperature region, followed by recovery and a subsequent increase at higher temperatures. This nonmonotonic behavior indicates that the density dependence of S_χ is intrinsically nontrivial.

The behavior of $S_\chi(T,\mu_q)$ can be understood as the result of competing effects summarized in Table 3. The chemical potential μ_q determines the fermionic occupation structure through the formation of a Fermi surface, driving a broad momentum region toward nearly idempotent occupation numbers ($n_\pm \simeq 0$ or 1) and thereby reducing the mixedness of the reduced chiral sector. By contrast, finite temperature thermally broadens the Fermi surface, leading to fractional occupation probabilities and increased mixedness.

The dynamical quark mass M_q provides an additional control through the Dirac structure of the correlator. A large M_q suppresses helicity-dependent mixing and reduces the spread of the eigenvalue spectrum, whereas a decreasing M_q weakens this suppression and allows stronger chirality mixing. The observed behavior of $S_\chi(T,\mu_q)$ is therefore governed by the interplay among Fermi-surface sharpening, thermal broadening, and mass-controlled chirality mixing.

The comparison between the chiral limit and the finite-mass case shows that a finite current quark mass smooths the overall structure of the entropy landscape. In the chiral limit, the variation of S_χ across the transition region is sharper, whereas for finite m_q the change becomes more gradual, consistent with the crossover nature of the transition in the mass sector.

To quantify the relationship between the entropy and the conventional mass-based indicator of chiral restoration, we compare the temperature derivatives of M_q and S_χ in Fig. 4. The extrema of $\mathrm{d}M_q/\mathrm{d}dT$ and $\mathrm{d}S_\chi/\mathrm{d}T$ do not coincide. At $\mu_q = 0$, the minimum of $\mathrm{d}M_q/\mathrm{d}T$ is located near $T \approx 187$ MeV, whereas the peak of $\mathrm{d}S_\chi/\mathrm{d}T$ appears near $T \approx 222$ MeV. At $\mu_q = 200$ MeV, the corresponding temperatures shift to approximately 140 MeV and 191 MeV, respectively.

This separation has a clear physical origin. The dynamical quark mass M_q probes the onset of symmetry restoration through the melting of the chiral condensate, whereas S_χ measures the subsequent development of mixedness in the fermionic subsystem, which requires sufficient thermal broadening. Consequently, the peak of $\mathrm{d}S_\chi/\mathrm{d}T$ is shifted to higher temperatures relative to the extremum of $\mathrm{d}M_q/\mathrm{d}T$.

In addition, Fig. 4(c) shows that $\mathrm{d}M_q/\mathrm{d}\mu_q$ is negative, indicating that increasing chemical potential weakens dynamical mass generation, whereas $\mathrm{d}S_\chi/\mathrm{d}\mu_q$ is positive and exhibits a broad maximum, reflecting the enhanced sensitivity of the entropy to density. This further demonstrates that S_χ does not track the mass sector on a point-by-point basis, but instead encodes both mass reduction and density-driven rearrangement of the occupation structure.

Overall, the chirality-reduced entropy provides a correlator-based diagnostic of the transition region in hot and dense quark matter. It is sensitive to both thermal broadening and density-induced occupation restructuring, thereby capturing information beyond conventional symmetry-breaking observables. All results are obtained within the mean-field NJL framework combined with the narrow-width quasiparticle approximation, where the entropy is computed from the equal-time correlation matrix of a Gaussian fermionic state.

VII. SUMMARY AND OUTLOOK

Our results show that chiral symmetry restoration and the mixedness of the chirality-reduced subsystem are closely related, but not identical, even in a mean-field QCD-like model. In this work, we developed a correlator-based framework for analyzing chiral-sector mixedness in hot and dense quark matter within the finite-temperature, finite-density Nambu–Jona-Lasinio (NJL) model. Start-

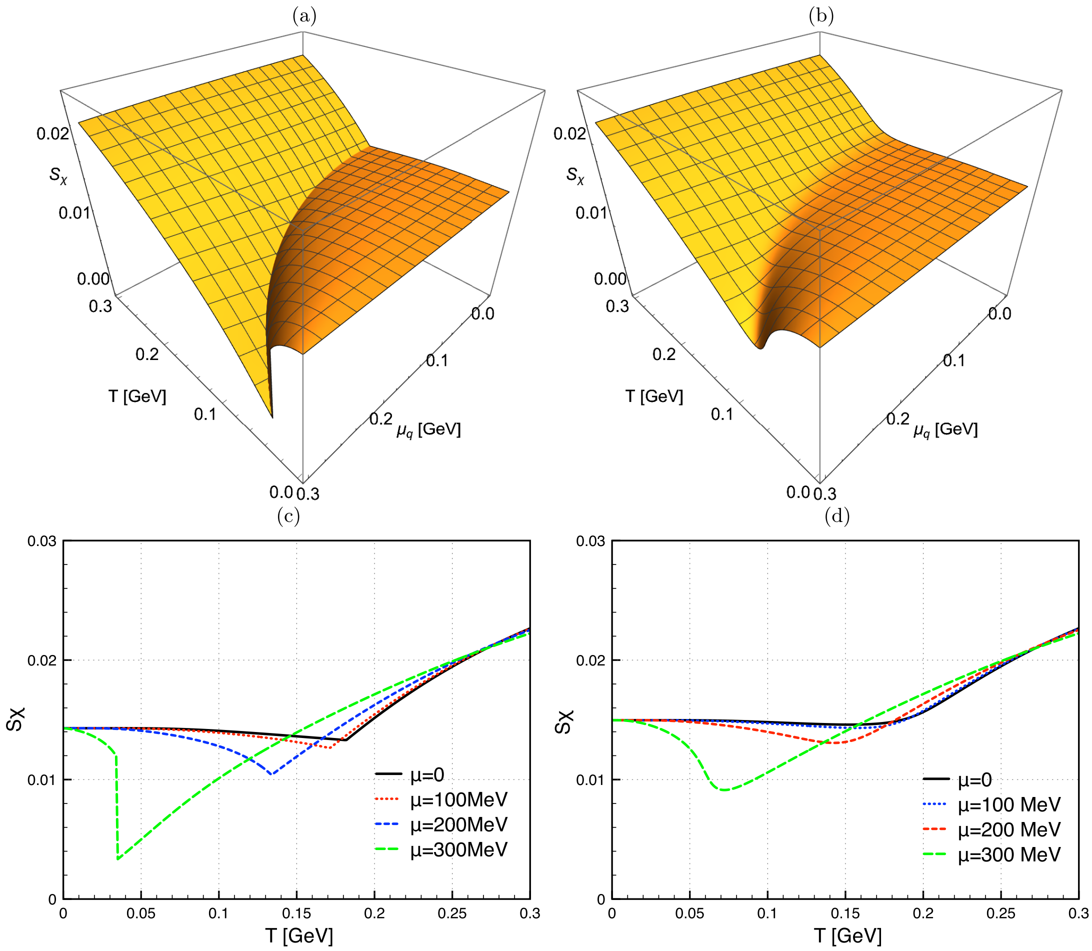

Fig. 3. (color online) Chirality-reduced entropy S_χ, defined in Eq. (22), as a function of temperature T and quark chemical potential μ_q for $m_q = 0$ in panel (a) and $m_q = 5.25$ MeV in panel (b). Panels (c) and (d) show the corresponding two-dimensional slices at fixed values of μ_q.

Table 3. The roles of temperature T, chemical potential μ_q, and dynamical mass M_q in determining the chirality-reduced entropy S_χ are governed by the competition among Fermi-surface sharpening, thermal broadening, and mass-controlled chirality mixing.

Parameter	Physical role	Tendency for S_χ
μ_q	Fixes fermionic occupation (Fermi-surface formation)	Suppresses
T	Induces thermal broadening (occupation smearing)	Enhances
M_q	Controls chirality mixing via the Dirac mass	Suppresses

ing from the lesser Green's function $G^<(k)$ in the real-time formalism, we constructed the equal-time correlation matrix $C(\boldsymbol{k})$ and defined the left-handed reduced correlator $C_L(\boldsymbol{k}) = P_L C(\boldsymbol{k}) P_L$. The corresponding von Neumann entropy, $S_\chi = -\mathrm{Tr}[C_L \ln C_L + (1-C_L)\ln(1-C_L)]$, was used to characterize the mixedness of the chirality-reduced subsystem. In this framework, the reduced correlator retains a nontrivial helicity structure and must therefore be described by its full eigenvalue spectrum rather than by a single scalar occupation probability.

The self-consistent solutions of the NJL gap equation reproduce the expected QCD-like chiral phase structure, featuring a second-order transition in the chiral limit and a smooth crossover for a finite current quark mass. Using these solutions, we evaluated the chirality-reduced entropy density S_χ/V and found that it exhibits nontrivial behavior across the chiral transition region. Although S_χ is correlated with chiral restoration, it is not an order parameter. Instead, it should be interpreted as a correlator-based measure of reduced chiral-sector mixedness that provides information complementary to the conventional chiral condensate through the full spectrum of the reduced correlator.

A central result of the present analysis is that the tem-

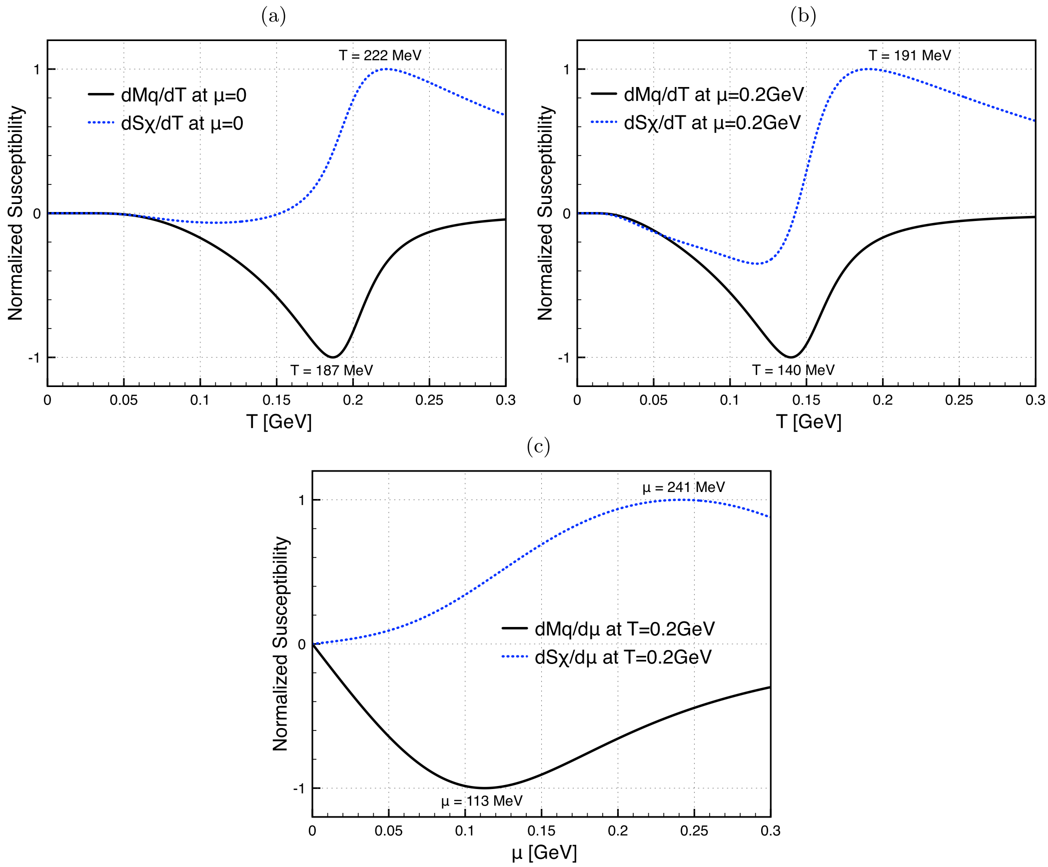

Fig. 4. (color online) Normalized responses of the dynamical quark mass and chirality-reduced entropy: $\mathrm{d}M_q/\mathrm{d}T$ and $\mathrm{d}S_\chi/\mathrm{d}T$ at $\mu_q=0$ (a) and $\mu_q=200$ MeV (b), and $\mathrm{d}M_q/\mathrm{d}\mu_q$ and $\mathrm{d}S_\chi/\mathrm{d}\mu_q$ at fixed temperature $T=0.2$ GeV (c). The extrema of the entropy response generally do not coincide with those of the dynamical mass response.

perature response of S_χ does not coincide with that of the dynamical quark mass. In particular, the peak of $\mathrm{d}S_\chi/\mathrm{d}T$ is shifted relative to the extremum of $\mathrm{d}M_q/\mathrm{d}T$, indicating that the development of reduced-sector mixedness and the rapid melting of the dynamical mass need not occur at the same temperature. At fixed temperature, the chemical-potential responses also show a clear separation between the mass and entropy sectors: while $\mathrm{d}M_q/\mathrm{d}\mu_q$ remains negative, $\mathrm{d}S_\chi/\mathrm{d}\mu_q$ is positive and develops a broad maximum at intermediate μ_q. These results show that the chirality-reduced entropy probes aspects of chiral dynamics that are not fully captured by conventional symmetry-breaking observables alone.

In this sense, the present study provides an internal chiral-subsystem counterpart to other information-theoretic approaches to QCD. Whereas spatial, partonic, or color-sector entropies probe different partitions of the QCD state, the present S_χ probes the reduced mixedness associated with chirality projection. This perspective also clarifies the limitation of the observable: S_χ is not a new order parameter for chiral symmetry restoration, but rather a correlator-based diagnostic that complements conventional condensate- and mass-based descriptions.

The present framework can be extended in several directions. It would be worthwhile to investigate how vector interactions, finite spectral widths, and beyond-mean-field non-Gaussian correlations modify the reduced correlator and its entropy. Extensions to PNJL-type or other confining frameworks would also allow one to study the interplay between deconfinement and chirality-reduced entropy in a more realistic setting. On the nonperturbative side, future lattice-QCD studies based on fermionic two-point functions and equal-time correlation matrices may help assess the extent to which chirality-projected reduced entropies can serve as robust information-theoretic probes of chiral dynamics in strongly interacting matter.

APPENDIX

A. Validity range of the equilibrium assumption

The equilibrium relations used in Eqs. (7) and (8)

$$G^<(p)=\mathrm{i}\,n_F(p^0)A(p),\quad G^>(p)=-\mathrm{i}[1-n_F(p^0)]A(p),\quad \text{(A1)}$$

are valid when the system is in local thermal equilibrium and its relaxation time $\tau_{\rm rel}$ is sufficiently long compared with the microscopic interaction time. In this regime, quasiparticle excitations are well defined, and the spectral function is sharply peaked near the mass shell,

$$A(p) \simeq 2\pi\,\mathrm{sgn}(p^0)\,\delta(p^2 - M_q^2), \tag{A2}$$

so that finite-width effects can be neglected. This narrow-width quasiparticle limit justifies the use of the on-shell expressions in Eqs. (9)–(13).

If a finite-width spectral function is retained, the equal-time correlator is still defined by

$$C(\boldsymbol{k}) = \mathrm{i}\int \frac{\mathrm{d}k^0}{2\pi} G^<(k), \tag{A3}$$

and the chirality-reduced correlator by

$$C_L(\boldsymbol{k}) = P_L C(\boldsymbol{k}) P_L = \mathrm{i}\int \frac{\mathrm{d}k^0}{2\pi} P_L G^<(k) P_L. \tag{A4}$$

Accordingly, S_χ quantifies the mixedness of the reduced chiral sector while accounting for possible broadening effects, and it reduces to the on-shell expression in Eq. (22) in the narrow-width limit. In this sense, finite spectral widths provide an additional source of reduced-sector mixedness associated with thermal smearing and quasiparticle damping.

B. Justification for using the equal-time reduced correlator

In equilibrium, the lesser Green's function $G^<(k)$ describes the occupied component of the single-particle spectrum, whereas the entropy of a Gaussian fermionic subsystem is determined by the corresponding equal-time correlation matrix. Accordingly, we define

$$C(\boldsymbol{k}) = \mathrm{i}\int \frac{\mathrm{d}k^0}{2\pi} G^<(k), \quad 0 \le C(\boldsymbol{k}) \le 1. \tag{B1}$$

For a Gaussian (mean-field) fermionic state, this correlator fully determines the state at the level of two-point correlations.

Projecting onto the left-handed subspace with $P_L = (1-\gamma^5)/2$, we obtain

$$C_L(\boldsymbol{k}) = P_L C(\boldsymbol{k}) P_L = \mathrm{i}\int \frac{\mathrm{d}k^0}{2\pi} P_L G^<(k) P_L. \tag{B2}$$

The matrix $C_L(\boldsymbol{k})$ is the reduced equal-time correlation matrix for the left-handed sector. Its eigenvalues satisfy

$$0 \le \lambda_\pm(\boldsymbol{k}) \le 1. \tag{B3}$$

Thus, they admit the standard fermionic probability interpretation and determine the entropy of the reduced Gaussian subsystem. The corresponding von Neumann entropy is

$$S_\chi = -\mathrm{Tr}\left[C_L \ln C_L + (1-C_L)\ln(1-C_L)\right]. \tag{B4}$$

Thus, within the mean-field or quasiparticle approximation, C_L is the appropriate object for constructing the entropy.

References

[1] Y. Nambu and G. Jona-Lasinio, Phys. Rev. **124**, 246 (1961)
[2] S. P. Klevansky, Rev. Mod. Phys. **64**, 649 (1992)
[3] T. Hatsuda and T. Kunihiro, Phys. Rept. **247**, 221 (1994)
[4] M. Buballa, Phys. Rept. **407**, 205 (2005)
[5] K. Fukushima and T. Hatsuda, Rept. Prog. Phys. **74**, 014001 (2011)
[6] Y. Aoki, G. Endrodi, Z. Fodor *et al.*, Nature **443**, 675 (2006)
[7] S. Borsanyi, G. Endrodi, Z. Fodor *et al.*, JHEP **11**, 077 (2010)
[8] C. Ratti, M. A. Thaler, and W. Weise, Phys. Rev. D **73**, 014019 (2006)
[9] K. Fukushima, Phys. Rev. D **77**, 114028 (2008) [Erratum: Phys. Rev. D **78**, 039902 (2008)]
[10] S. i. Nam, J. Phys. G **37**, 075002 (2010)
[11] V. Vedral, Rev. Mod. Phys. **74**, 197 (2002)
[12] L. Amico, R. Fazio, A. Osterloh *et al.*, Rev. Mod. Phys. **80**, 517 (2008)
[13] P. Calabrese and J. Cardy, J. Phys. A **42**, 504005 (2009)
[14] H. Casini and M. Huerta, Phys. Rev. D **90**(10), 105013 (2014)
[15] D. E. Kharzeev and E. M. Levin, Phys. Rev. D **95**(11), 114008 (2017)
[16] K. Zhang, K. Hao, D. E. Kharzeev *et al.*, Phys. Rev. D **105**(1), 014002 (2022)
[17] M. Hentschinski, D. E. Kharzeev, K. Kutak *et al.*, Rept. Prog. Phys. **87**(12), 120501 (2024)
[18] M. Levin and X. G. Wen, Phys. Rev. Lett. **96**, 110405 (2006)
[19] S. Ryu and T. Takayanagi, Phys. Rev. Lett. **96**, 181602 (2006)
[20] S. i. Nam, Phys. Rev. C **113**(1), 015203 (2026)
[21] L. P. Kadanoff and G. Baym, *Quantum Statistical Mechanics* (W. A. Benjamin, New York, 1962)
[22] L. V. Keldysh, Sov. Phys. JETP **20**, 1018 (1965)